

KINEMATIC APPROACH FOR A GLOBAL-LOCAL COUPLING: COMPRESSIVE BEHAVIOUR OF A DELAMINATED PANEL

R. Borrelli^{1*}, F. Caputo², A. Riccio², F. Scaramuzzino², A. Sellitto²

¹Italian Aerospace Research Centre (CIRA), Aerostructural Design and Analysis Lab., Italy

²Second University of Naples, Aerospace and Mechanics Engineering Department, Italy

*Author to whom correspondence should be addressed: E-mail: r.borrelli@cira.it, +39 0823 623 544

Received 6 July 2011; accepted 28 July 2011

ABSTRACT

A kinematic approach to global/local coupling has been applied to investigate the behaviour of a delaminated stiffened composite panel, by using an in-house finite element based procedure. The delamination growth phenomenon has been simulated by employing fracture elements implemented in the B2000++[®] code, which are based on the Modified Virtual Crack Closure Technique (MVCCT); this technique is able to compute the energy release rate on the delamination front for each fracture mode. A very fine three-dimensional mesh in the delaminated region has been considered in order to obtain a good prediction of the delamination growth. The rest of the structure has been modelled by means of shell elements. A global/local approach based on point-wise multipoint constraint has been implemented in the in-house-code and used to connect shell meshes to solid ones. A numerical application on a delaminated composite stiffened panel taken from literature has been introduced. Models characterized by different levels of complexity, i.e. without delamination, with delamination, with delamination growth have been considered and compared to understand the effectiveness of the introduced kinematic approach.

Keywords: Global/Local; MPC; MVCCT; B2000++; delamination growth.

1. INTRODUCTION

The demand for composite materials is continuously increasing among aerospace industries, but the prediction of their mechanical behaviour has not yet gained satisfying level of robustness and reliability. This is principally due to the uncertainties related to the peculiar damage phenomenologies characterizing composite materials, involving different types of failure modes which interact with each other. One of most common and dangerous failure modes of composite structures is the delamination one, which has an important effect on the reduction of the global stiffness of a laminate and can create a local instability, which may lead to a compressive failure. Therefore, an accurate prediction of residual stiffness and strength of delaminated structures under compressive loads is needed.

The main objective of this work has been to investigate and predict the behaviour of a stiffened delaminated composite panel through the use of a finite element based procedure. In order to simulate the delamination growth, fracture elements implemented in B2000++[®] 1 code, within the frame of previous research activities (2-4), have been employed. Intralaminar damage, in the form of matrix crack-

ing and fibre failure, has not been taken into account in our model, although at the level of strain applied in this analysis, such damage modes may affect the global response of the panel, as was found in 5, 6 and 7. The B2000++[®] fracture elements are based on the Modified Virtual Crack Closure Technique (MVCCT, 8), by which it is possible to numerically compute the energy release rate on the delamination front for each fracture mode. An empirical delamination growth criterion based on the computed energy release rate and on the critical material toughness is then applied. Fracture elements are placed at the interface between two surfaces initially undelaminated. If this criterion is fulfilled in a generic location of the delamination front, fracture elements release nodes in that location, allowing the separation of the two surfaces. The MVCCT, thanks to the hypothesis of small delamination changes for each time step 8, allows computing forces and displacement at the delamination tip in the same analysis hence allows performing the delamination growth analysis with a single computation for each time step. This would not be possible with the traditional VCCT which needs two different analyses, for the computation of forces and displacements at the delamination tip respectively, for each time step.

Since the energy release rate is a function of both the forces at the crack tip and the crack opening displacement (COD), a very fine three-dimensional mesh is required for the good prediction of these quantities. On the other hand, a fine 3D discretization of complex structures is not suitable due to the increasing of the calculation time. Hence, with the aim of extending the field of applicability of the damage prediction tool to geometrically complex structures, a global/local approach has been used. In particular, a shell/3D modelling approach (9-10), for which a local three-dimensional solid finite element model, which represents the area of interest and where a detailed stress distribution evaluation is required, has been used only very close to the delaminated area, while a 2D-shell model has been used for the areas of minor interest. In such a manner the accuracy of a three-dimensional model has been combined with the computational efficiency of a shell finite element model. In order to couple the shell domain to the solid one, shell-to-solid coupling elements based on kinematic constraints and available in the finite element code B2000++[®] have been used. B2000++[®] offers the capability to implement new elements and new solver routine (written in FORTRAN and C++). The new elements are not user subroutines but elements ex novo based on the same architecture of native elements in B2000++[®]. The code offers also the capability to manage data through a robust database manager which allows the handling of complex models with a relevant number of degrees of freedom. In other words B2000++[®] can be considered a fully customizable research oriented FEM code with a specific different target (research) with respect to commercial FEM code. This is the reason why this code has been adopted for the developments presented in this paper, which is aimed to provide a computational effective delamination growth approach fully integrated in the FEM code and able to be adopted for large and complex structural configurations.

2. TEST CASE DESCRIPTION

The proposed finite element procedure has been applied to a literature test case carried out from 11 and 12. As shown in Fig. 1, it consists of a carbon-fibre reinforced panel stiffened by three I-section stringers and with an initial circular delamination located at the centre of the bay and placed between the fifth and the sixth ply in the thickness of the skin. The stacking sequence of the skin was $[(+45^\circ/-45^\circ/0^\circ/90^\circ)]_{4s}$, while each stringer was made of 4 laminates, each one with the following lay-up $(-45^\circ/+45^\circ/0^\circ)_{2s}$. According to the Fig. 1, the 0° direction is the parallel

one to the y axis.

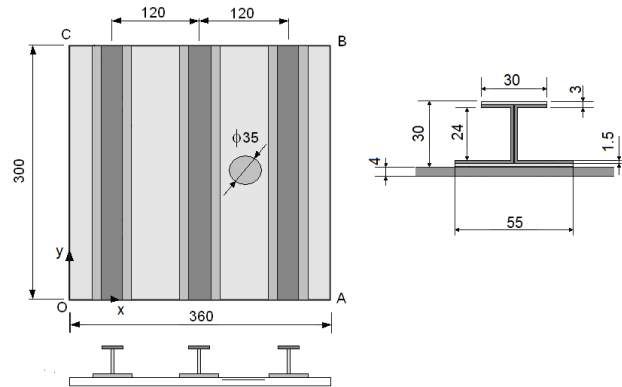


Fig. 1: Geometrical description of the test case 12 units in mm

The material properties of the adopted composites (T800/924) are summarized in Table 1 13.

Table 1: Material properties of the composite lamina

Property	Average (Cv)
Longitudinal Young's modulus, E_{11} (GPa)	155.21 (7%)
Transverse Young's modulus, E_{22} (GPa)	8.57 (3%)
Normal Young's modulus, E_{33} (GPa)	8.57 (3%)
In-plane shear modulus, G_{12} (GPa)	7.40 (5%)
Out-of-plane shear modulus, G_{13} (GPa)	7.40 (5%)
Out-of-plane shear modulus, G_{23} (GPa)	7.40 (5%)
Poisson's ratio, ν_{12}	0.36
Poisson's ratio, ν_{13}	0.36
Poisson's ratio, ν_{23}	0.36
Critical Energy release rate mode I, G_{IC} (J/m ²)	280
Critical Energy release rate mode II, G_{IIC} (J/m ²)	575
Ply thickness (mm)	0.125

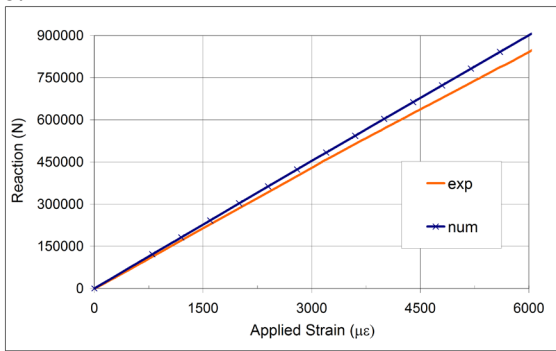
The experimental test has been performed under displacement control: the edge BC of the panel has been clamped while on the opposite edge (OA) a uniform displacement along the y-axis has been applied. The rotation on the edge OA is not allowed and the lateral edges (OC and AB) are free.

3. NUMERICAL RESULTS

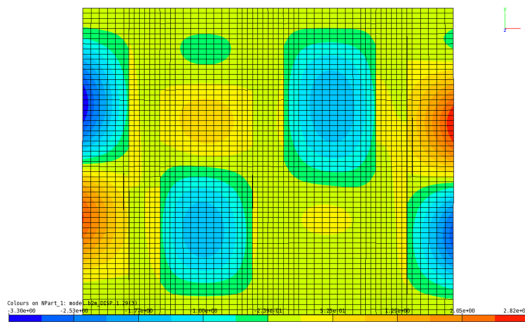
In order to predict the compressive behaviour of a stiffened panel by taking into account the evolution of an embedded defect, as a delamination one, non linear static finite element analyses have been performed. Three modelling approaches have been adopted in order to progressively take into account the presence of complex phenomena such as local instabilities and delamination growth. Basically, three FE models (which hereafter will be called S1, S2 and S3) have been created.

Model S1: in this FE model each component of the stiffened panel (skin, base stringer, web and top stringer) has been modelled by a single layer of shell elements, therefore, the local effects due to the presence of the embedded delamination have been

not yet considered. This first step is needed to assess the capability of the FE model in reproducing accurately the global stiffness of the panel under compressive load. A sensitivity mesh analysis has been performed with the aim at evaluating the effects of the mesh refinements on the results. The correlation between the experimental 12 and the numerical reaction force vs. applied strain is good (Fig. 2a). Finally, the predicted buckling mode is shown in Fig. 2b.



a)



b)

Fig. 2: a) Reaction vs. Applied strain curve, b) Buckling mode

Model S2: in this second step, the area surrounding the delamination that is the area of interest, has been modelled by two layers of solid elements, while all the other regions have been still modelled by means of shell elements. The modelling approach is sketched in Fig. 3 which represents a section along the plane $y=150\text{mm}$: indeed, because of the presence of the initial circular delamination (MN) between the 5th and the 6th ply, the laminate can be divided into a lower sublaminate (3.375mm thick) and into an upper one (0.625mm thick). The first layer of solid elements, which is the thickest one, is representative of the plies below the delamination plane (lower sublaminate, where the stringers side of the panel is the upper one), while the second layer, which is the thinnest one, is representative of the plies above the delamination plane (upper sublaminate). It is worth to notice that the position of delamination between the 5th and the 6th ply has been

arbitrary set and it is representative of a damage induced by a low velocity impact on the panel. Since only a delamination growth model and no criterion for the on-set of delamination are introduced in this paper, it is assumed that an initial circular delamination is already present at the beginning of the analysis, without questioning on the origin (in terms of location and energy of the impact) of delamination self.

Contact elements have been placed on the initial delaminated area in order to avoid penetrations which could occur during the load application. A node to node penalty formulation has been adopted to reduce the computational effort. From the results of the analysis a penalty factor of $1.0e3$ has been used which was found able to return negligible penetration between contacting surfaces.

At this step, no fracture elements were introduced into the model and the delamination growth is not yet simulated in this model.

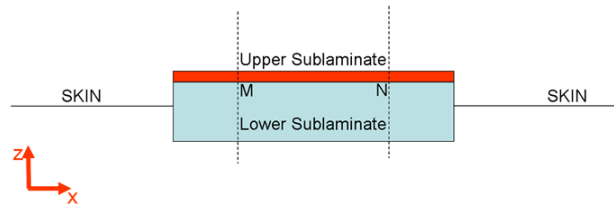


Fig. 3: Modelling approach

Shell and solid elements have been connected by using shell-to-solid coupling elements based on kinematic constraints between the degrees of freedoms of the nodes which are located at common boundaries. Such coupling elements are able to couple the shell region to the solid one, even if they have been discretized with different mesh densities. In order to take advantage from this capability, within the context of model S2, two different models have been generated with two different solid mesh densities (MD1 and MD2), as shown in Fig. 4.

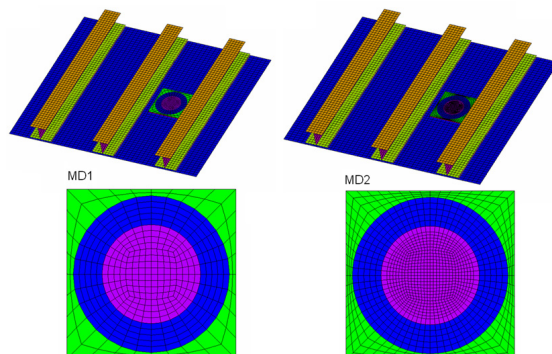


Fig. 4: S2 Model with 2 different solid mesh densities

In Fig. 5, the numerical reaction force vs. applied strain curves are compared to the experimental one. Both the curves obtained by model S2 (MD1 and MD2) overlap the curve obtained by model S1, therefore, the introduction of the solid region into the model doesn't changed the stiffness of the panel.

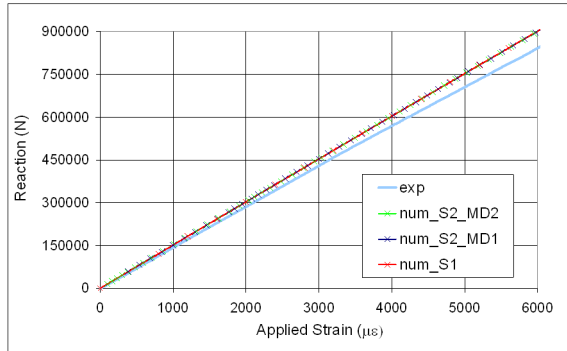


Fig. 5: Comparison between experimental and numerical reaction vs. applied strain curve

Unlike model S1, model S2 allows to simulate the local buckling, that is the local instability of the upper and thinnest sublaminates. As matter of the fact, in Fig. 6 the out of plane displacements (computed at the centre of delamination) vs. applied strain curves are plotted for the lower and the upper sublaminates. It was found that at about 1900µε the upper sublaminates suddenly separates from the lower one. At the local buckling load, the instability is detected only in the delaminated region (this is confirmed by the out of plane displacement contour plot of Fig. 7, which refers to an applied strain of 1954µε) and the out of plane displacement of the thin sublaminates starts to be positive. This displacement value increases with the load value, up to the global buckling condition, when the whole panel is interested by instability phenomenon (Fig. 8). By then, the thin sublaminates is obliged to follow the buckle shape of the skin, which causes a decrease in the out of plane displacement.

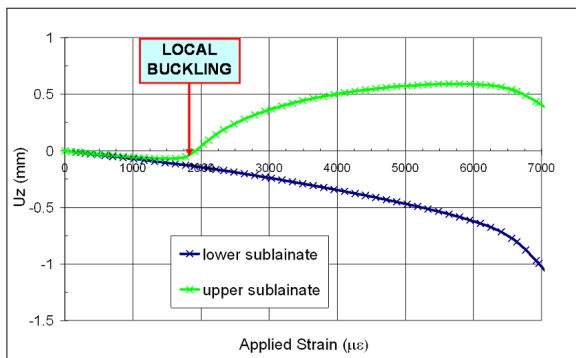


Fig. 6: Out of plane displacement (centre of delamination) vs. applied strain

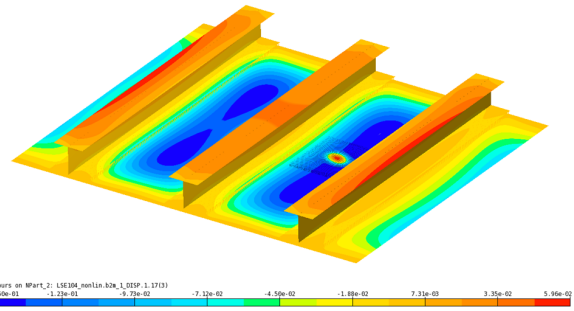


Fig. 7: Out of plane displacement contour plot at 1954µε

Finally, the continuity of the displacement field along the interface between the shell region and the solid one has been verified as shown in the out of plane displacement contour plot of Fig. 8.

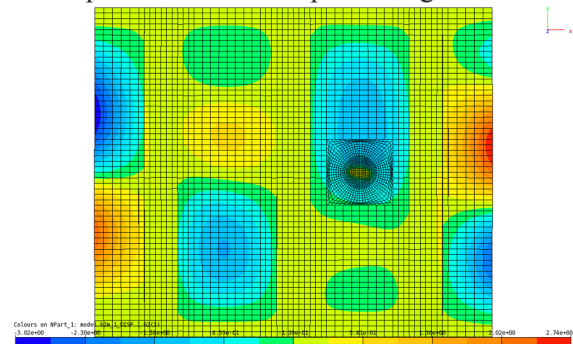


Fig. 8: Out of plane displacement contour plot – global buckling condition

Model S3: as a last step, fracture elements based on the MVCC technique have been introduced into the model, allowing the delamination growth to be simulated. In the FE model S3, three different zones can be distinguished within the solid area. According to the Fig. 9, where a quarter of the solid finite element model is shown, the three zones are the following ones:

Zone I: is the initial delaminated area; as well as in model S2, contact elements are needed between the two sublaminates in order to avoid penetration;

Zone II: is the zone where the delamination can grow. Fracture elements are introduced at the interface between the upper and the lower sublaminates. They connect a node of the upper sublaminates with a corresponding node of the lower sublaminates and the connection between the two nodes is released when the linear delamination growth criterion in the following Eq. (1) is fulfilled;

$$\frac{G_I}{G_{IC}} + \frac{G_{II}}{G_{IIC}} + \frac{G_{III}}{G_{IIIC}} = 1 \quad (1)$$

Other kinds of delamination growth criteria are available in literature. A complete review for them is available in 14. However, in our investigation, the linear delamination growth criterion (Eq. (1)) has been used, which though very simple, provided good results in previous research works 4, 15. In the case of this embedded circular delamination the contribution of mode III seems to be negligible if compared to the other two modes as was found in 4, 16, 17, since no torsional effect after delamination buckling can be appreciated. Moreover, the results obtained in 18, 19, 20 show that the value of G_{IIIc} is usually much higher than G_{IIc} which imply a lower weight of mode III in equation 1. Our analysis, performed using a $G_{IIIc}=G_{IIc}$, confirmed that mode III contribution to ERR is negligible with respect to mode I and mode II.

Zone III: is the zone where the solid mesh is connected to the shell mesh. The nodes at the interface between the two sublaminates have been “merged”, therefore, the delamination is not allowed to grow in this zone.

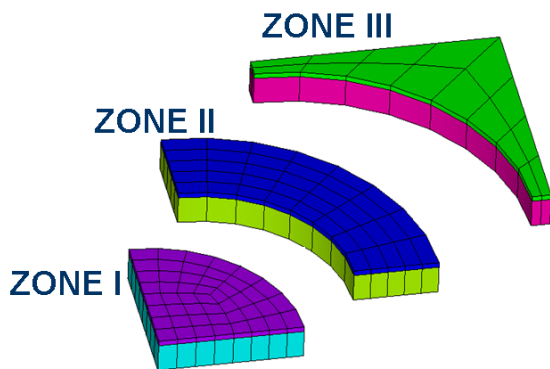


Fig. 9: Distinguishable Zones of the embedded solid finite element model

In Fig. 10, the out of plane displacement of the lower sublaminates, computed at the centre of the delamination, is plotted as function of the applied strain for each of the investigated FE models. It was found that global buckling load, computed as the intersection between the tangents to the curves at their end points, is quite influenced by the local events. In particular, the global buckling load happens early if the local buckling and, above all, the delamination growth are simulated. The evolution of the damage is shown in Fig. 11. At about $1800\mu\epsilon$ the upper sublaminates starts to separate from the lower one (local buckling). The delamination starts to grow at about $3190\mu\epsilon$ (delamination initiation strain) and propagates quite quickly. It was found a small angle between the propagation direction and the plane

$y=150\text{mm}$. Such result was found consistent with the experimental behaviour, as shown in Fig. 12, where the numerical and experimental out-of-plane distributions at $3530\mu\epsilon$ are compared. An image of the delaminated area at $4069\mu\epsilon$ is shown in the out-of-plane displacement contour plot of Fig. 13.

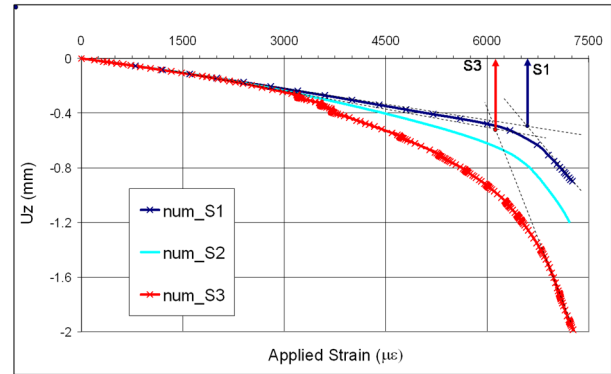


Fig. 10: Out of Plane displacement (centre of delamination) vs. applied strain curve

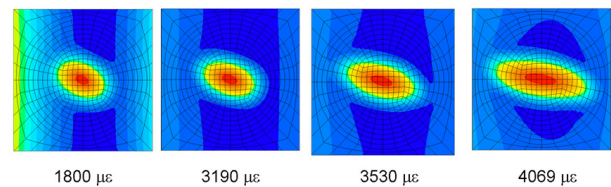


Fig. 11: Evolution of delamination growth

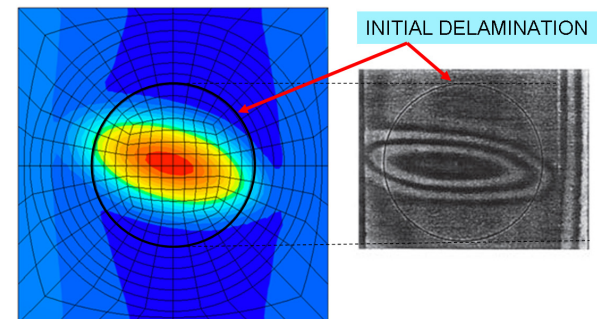


Fig. 12: Comparison between numerical and experimental out-of-plane distribution at $3530\mu\epsilon$.

Finally, in Fig. 14, the numerical values are compared with available experimental data 11 in terms of global buckling load and delamination initiation strain. The FE model S3 was found able to predict both the global buckling load with a maximum error of 4.4% and the delamination initiation strain with a maximum error of about 8.8%.

4.CONCLUSIONS

In this article, a global/local approach (shell/3D) has been used to investigate on the compressive behaviour of a stiffened composite panel, on which a bay

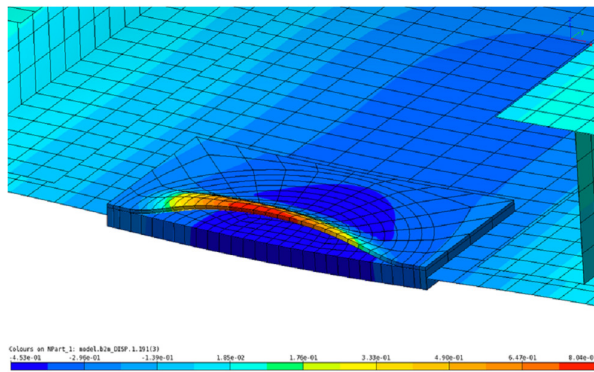


Fig. 13: Out of plane displacement contour plot for the delaminated area at 4069 $\mu\epsilon$

delamination is present. In particular, a local refined 3D model used to simulate the local buckling and the delamination growth, has been coupled with a global courser shell model by using shell-to-solid coupling elements based on kinematic constraint. Fracture elements based on the MVCC technique have been used to simulate the delamination propagation.

Basically, three modelling approaches (S1, S2 and S3) have been developed in order to increase gradually the complexity of the proposed FE models. It was found that the prediction of the global buckling load improves if local instability and the delamination growth is simulated (model S3). Moreover, the delamination initiation load is predicted with a good accuracy by the model S3.

The proposed model does not take into account the effect of the intralaminar damage (matrix/fibre failure), which may occur during the compression condition and which may affect the residual stiffness and strength of the panel. Authors intend to include such effects to improve the model in the future research work.

ACKNOWLEDGMENTS

Authors would like to kindly thanks Dr. Ludwig Thomas from SMR Engineering for his precious technical support and assistance with the finite element code B2000++®. The authors would like also to acknowledge the support provided by Dr Emile Greenhalgh with the experimental data needed to validate the model proposed in this work. The research leading to these results was carried out within the project “generic linking of Finite Element based Models - gIFEM” which has received funding by the European Community’s Seventh Framework

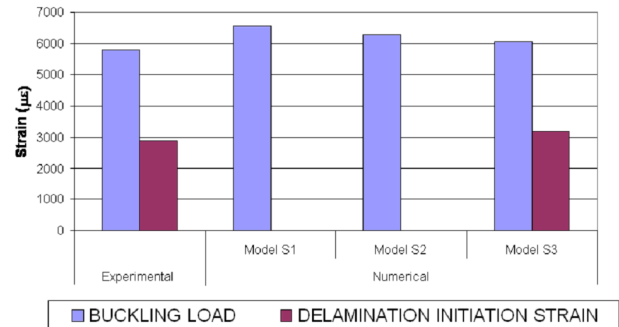


Fig. 14: Comparison between numerical and experimental data 11

Programme (FP7/2007-2013) under the grant agreement n° 234147.

References:

1. The B2000++ User Manual, SMR Engineering & Development SA, 2011. http://www.smr.ch/local/doc/B2000++/user_manual/index.html
2. **Riccio, A., Perugini, P., Scaramuzzino, F.** “Modelling Compression Behaviour of Delaminated Composite Panels”, *Computers & Structures*, **78/73-81** (2000). ISSN: 0045-7949.
3. **Riccio, A., Perugini, P., Scaramuzzino, F.** “Embedded Delamination Growth in Composite Panels under Compressive Load”, *Composites part B: Engineering*, **32/3**, 209-218 (2001). ISSN: 1359-8368.
4. **Riccio, A., Perugini, P., Scaramuzzino, F.** “Influence of Contact Phenomena on Embedded Delamination Growth in Composites”, *AIAA Journal*, **41/5**, 933-940 (2003). ISSN 0001-1452.
5. **Berbinau, P., Soutis, C. and Guz, I. A.** “Compressive failure of 0° unidirectional CFRP laminates by fibre microbuckling”, *Composites Sci. & Technol.*, **59/9**, (1999), 1451-1455.
6. **Zhuk, Y., Guz, I.A. and Soutis, C.** “Compressive behaviour of thin-skin stiffened composite panels with a stress raiser”. *Composites Part B*, **32/8**, (2001), 697-709.
7. **Koundouros, M., Falzon, B., Soutis, C and Lord, S. J.** “Predicting the ultimate load of a CFRP wing-box”. *Composites A*, **35/7-8**, (2004), 895-903.
8. **Krueger R.** “The Virtual Crack Closure Technique: History, approach and application”, *NASA/CR-2002-211628* (2002).
9. **Alesi, H., Nguyen, V. M., Mileshkin, N.,** “Global/Local Postbuckling Failure Analysis of Composite Stringer/Skin Panels”, *AIAA Journal* **36/**. 9 (1998).
10. **Krueger, R., O’ Brien T. K.,** “A Shell/3D Modelling Technique for the Analysis of Delaminated Composite Laminates”, *Composites: Part A*, **32** (2001) 25-44.

11. **Greenhalgh, E., Singh, S., Nilsson, K. F.**, “Mechanisms and Modelling of Delamination Growth and Failure of Carbon-Fibre Reinforced Skin-Stringer Panels”, *Composite Structures: Theory and Practice*, ASTM STP 1383, Philadelphia, PA (2000).
12. **Riccio, A., Giordano, M., Zarrelli M.**, “A linear Numerical Approach to Simulate the Delamination Growth Initiation in Stiffened Composite Panels”, *Journal of Composite Materials*, **44/15**, 1841-1866 (2010).
13. **Greenhalgh, E.**, “Characterization of mixed-mode delamination growth in carbon-fibre composites”, PhD Thesis, Imperial College, London, 1998.
14. **Orifici, A.C. Herszberg, I., Thomson, R.S.**, “Review of methodologies for composite material modeling incorporating failure”, *Composite Structures*, **86**, 194-210, 2008.
15. **Gaudenzi, P., Perugini, P., Riccio, A.**, “Post-buckling behaviour of composite panels in the presence of unstable delaminations”, *Composite Structures*, **51**, 301-309, 2001.
16. **Singh, K.L., Dattaguru, B., Ramumurthy, T.S., Mangalgiri, P.D.**, “Delamination tolerance studies in laminated composite panels”, *Sadhana*, **25/4**, 409-422, 2000.
17. **Whitcomb, J.D.**, “Three dimensional analysis of a postbuckled embedded delamination”, *International journal of composite materials*, **23**, 862-889, 1989.
18. **de Morais, A.B., Pereira, A.B., de Moura, M.F.S.F.**, “Mode III interlaminar fracture of carbon/epoxy laminates using the six-point edge crack torsion (6ECT)”, *Composites: part A*, **42**, 1793-1799, 2011.
19. **de Morais, A.B., Pereira, A.B.**, “Mixed mode II + III interlaminar fracture of carbon/epoxy laminates”, *Composites science and technology*, **68**, 2022-2027, 2008.
20. **Wang, W.X., Nakata, M., Takao, Y., Matsubara, T.**, “Experimental investigation on test methods for mode II interlaminar fracture testing of carbon fibre reinforced composites”, *Composites: part A*, **40**, 1447-1455, 2009.